Journal of Catalysis **201,** 89–99 (2001)
doi:10.1006/jcat.2001.3228, available online at http://www.idealibrary.com on IDEAL®

# Reduction of $NO_x$ with Ammonia over Fe/MFI: Reaction Mechanism Based on Isotopic Labeling

Qi Sun, Zhi-Xian Gao, Hai-Ying Chen, and Wolfgang M. H. Sachtler[1]

*V. N. Ipatieff Laboratory, Center for Catalysis and Surface Science, Department of Chemistry, Northwestern University, Evanston, Illinois 60208*

Received December 8, 2000; revised March 12, 2001; accepted March 12, 2001; published online May 24, 2001

**The selective catalytic reduction of nitrogen oxides has been studied in the presence of $O_2$ over Fe/MFI catalysts with Fe/Al ∼ 1, prepared by sublimation of $FeCl_3$ vapor onto HMFI. Reduction of $NO_x$ is much faster with $NH_3$ than with isobutane. A 100% $NO_x$ reduction to $N_2$ is observed for an $NH_3$/NO ratio above unity and 90% for a 1/1 dosage. The catalyst is very active and stable in the presence of water vapor. Isotopic labeling with $^{15}NO$ shows that the preferred path for the reduction of $NO_x$ with $NH_3$ is via $NH_4NO_2$. This nitrite decomposes to $N_2 + 2H_2O$. A 100% pure $^{15}N^{14}N$ product is obtained by circulating a 1/1 mixture of $^{15}NO$ and $^{15}NO_2$ over a catalyst covered with adsorbed $^{14}NH_3$. In contrast, $^{14}N_2$ is formed by oxidation of $^{14}NH_3$ with $O_2$ or $N_2O_x$ with $x > 3$. The high efficiency of this catalyst is due to the fact that ammonia swiftly intercepts the oxidation of NO when the value of $x = 3$ is reached. At high temperature when little adsorbed water is present, water vapor promotes activity because it is needed for the formation of ammonium nitrite. At low temperature it acts kinetically as a mere competitor for the active sites.** © 2001 Academic Press

*Key Words:* **catalytic reduction of $NO_x$ with ammonia; Fe/MFI (Fe/ZSM-5) catalyst; sublimation technique; ammonium nitrite intermediate.**

## 1. INTRODUCTION

The selective catalytic reduction (SCR) with ammonia of nitrogen oxides, $NO_x$, in the emission from stationary sources has been widely studied. Vanadium catalysts have been developed and successfully commercialized. Kinetic studies have resulted in proposed reaction mechanisms (1–5). Concerns about the toxicity of vanadium motivated research for alternative SCR catalysts, in particular after the discovery by Iwamoto *et al.* (6) of zeolite-based catalysts, such as Cu/MFI.[2] Research of SCR with ammonia over this class of catalysts has been summarized by Centi and Perathoner (7) and Fritz and Pitchon (8).

With Fe/MFI there is a general consensus that high Fe loadings are desirable, with a concentration ratio of Fe/Al ∼ 1, where Al stands for the number of Al-centered tetrahedra in the zeolite lattice (9–11). Such catalysts have been obtained by a procedure in which sublimation of $FeCl_3$ vapor onto the H form of the zeolite is an important step. Co/MFI catalysts have been prepared by a variety of techniques, including ion exchange from aqueous solution (12), solid-state ion exchange (13), and sublimation of a Co halide onto HMFI (14). With isobutane 100% conversion to $N_2$ has been found. These catalysts also reduce $NO_x$ with methane.

Evidence has been obtained that an adsorption complex, $NO_y$, is formed on such catalysts with the nitrogen in an electrochemical valency ≥4. Work with Fe/MFI shows that such a complex reacts with the hydrocarbon to form a deposit, $C_xH_yN_z$, which reacts further with $NO + O_2$ or $NO_2$ to form $N_2$ (15). Isotopic labeling revealed that one N atom of the $N_2$ product stems from the $C_xH_yN_z$ deposit, the other from impinging NO or $NO_2$. From a comparison of the reaction rates with those of model compounds, it is concluded that during the formation of the $C_xH_yN_z$ deposit the N atoms are reduced to an electronegative state such as an amino group, $-NH_2$ (16). This transformation might include isocyanate or cyanide intermediates, for which other authors obtained spectroscopic evidence on similar catalysts (17–21).

As the reactivity of a C-bonded amino group will be similar to that of an adsorbed ammonia molecule, these observations suggest a mechanistic commonality of the SCR of nitrogen oxides with ammonia or a hydrocarbon as the reductant. A number of steps will be necessary to transform an oxygen-carrying N atom into an amine or amine-like group. These steps will be bypassed when the hydrocarbon in the feed is replaced by ammonia. It is therefore of interest to compare MFI-supported metal ions as catalysts for $NO_x$ reduction with isobutane and ammonia.

For Cu/MFI it is known that isolated $Cu^{2+}$ ions, $[Cu–O–Cu]^{2+}$ oxo-cations, and CuO particles can coexist in ion-exchanged Cu/MFI under oxidizing conditions (22–24). Among these the binuclear oxo-cation $[Cu–O–Cu]^{2+}$ is known to catalyze the oxidation of NO to $NO_2$. Likewise for Fe/MFI, prepared by sublimation of $FeCl_3$, numerous

---

[1] To whom correspondence should be addressed. Fax: (847) 467-1018. E-mail: wmhs@northwestern.edu.

[2] The MFI zeolite is often called ZSM-5.

data support the model that a binuclear oxo-ion, $[HO–Fe–O–Fe–OH]^{2+}$, is responsible for the high activity and selectivity in SCR of $NO_x$ with hydrocarbons (25–27). For $NO_x$ reduction to $N_2$ by isobutane in a gas flow with a space velocity GHSV of $4.2 \times 10^4\ h^{-1}$, Chen *et al.* (10) report a conversion to $N_2$ exceeding 70% at a temperature near 350°C. With an Fe/MFI catalyst prepared by a modified sublimation technique but ammonia as reductant, Ma and Grünert report 75–85% conversion of NO at a space velocity of $3.0 \times 10^4\ h^{-1}$. They also report a promoting effect of water and a much wider temperature window of high conversion (350–480°C) over Fe/MFI than over Cu/MFI (28).

Long and Yang claim 100% NO conversion with a feed containing equimolar concentrations of NO and $NH_3$ over Fe/MFI prepared by ion exchange (29). No explanation has been published for this nontrivial 1/1 consumption ratio of NO and $NH_3$. If NO is *not* oxidized to $NO_2$ and $NH_3$ does *not* react with $O_2$, one would obtain $F = [NO]/[NH_3] = 1.5$ for the reaction

$$3NO + 2NH_3 \rightarrow 2.5N_2 + 3H_2O. \qquad [1]$$

However, if NO oxidation to $NO_2$ is fast in an excess of $O_2$ and if $NO_2$ is the sole reactive oxidant, one would get $F = [NO]/[NH_3] = 0.75$ for

$$3NO_2 + 4NH_3 \rightarrow 3.5N_2 + 5H_2O. \qquad [2]$$

The value, $F = 1$, reported by Komatsu *et al.* (24) and Long and Yang (29, 30) could mean either a combination of [1] with an $NH_3$ combustion coincidentally consuming 50% of the $NH_3$ consumed in [1], or a new mechanism with predominant reaction of ammonia with nitrogen in an oxidation state of 3+, as in dinitrogen trioxide ($N_2O_3$) or $HNO_2$. For instance,

$$HNO_2 + NH_3 \rightleftharpoons NH_4NO_2 \rightarrow N_2 + 2H_2O. \qquad [3]$$

To identify the reaction mechanism, the present study makes extensive use of $^{15}N$-labeled nitrogen oxides.

Another incentive for this study is the clarification of the promoting effect of water on the $NO_x$ reduction with ammonia. Long and Yang (29) suggest that water increases the acidity of the catalyst, which they consider crucial for its activity (29–31). This is, however, in contradiction with our observations and the fact that, in an atmosphere with $NH_3$, the acid sites will be covered with adsorbed ammonia molecules, i.e., most acid sites will be neutralized.

In the present work, overexchanged Fe/MFI catalysts, prepared by $FeCl_3$ sublimation, were used as catalysts for SCR of $NO_x$ by ammonia. Identical conditions were used for $NO_x$ reduction with ammonia or isobutane. Isotopic labeling has been used to identify the origin of the two N atoms in the $N_2$ product. Adsorbates have been identified by *in situ* FTIR and by TPR.

## 2. EXPERIMENTAL

### 2.1. *Catalyst Preparation*

Fe/MFI catalysts were prepared by chemical vapor deposition; the details have been described previously (10). Na/MFI (provided by UOP Lot No. 99499506001, Si/Al = 19.0, Na/Al = 0.67) was first transformed to H/MFI by conventional ion exchange with a diluted ammonium nitrate solution, followed by calcination in an $O_2$ flow at 550°C for 4 h. $FeCl_3$ (Aldrich, 97%) was sublimed onto HMFI, so that all protons were consumed by

$$H^+ + FeCl_3 \rightarrow [FeCl_2]^+ + HCl \uparrow . \qquad [4]$$

The precursor was washed with distilled, deionized water to replace chloride ions by hydroxide ions, followed by calcination in flowing $O_2$ at 550°C for 4 h. Elemental analysis by inductively coupled plasma (ICP) atomic emission shows that the Fe/Al ratio is unity. FTIR confirmed that the intensity of the IR band at $3610\ cm^{-1}$, indicative of Brønsted acid sites, vanished after sublimation. During subsequent washing, some hydrolysis of the metal ions takes place, giving Brønsted sites. After this washing the intensity of the $3610\ cm^{-1}$ band amounted to 20% of the value of the parent HMFI.

### 2.2. *SCR of $NO_x$ by Ammonia and Isobutane*

Catalytic tests were carried out in a continuous-flow tubular fixed-bed microreactor as described previously (10). A 25-mg powder Fe/MFI sample was packed into a quartz reactor (i.d. 4 mm) with a porous frit and pretreated in a flowing premixed $O_2$/He (10.0%) flow of 100 mL/min (NTP) for 10 h at 500°C. After this treatment the reactor was cooled to the desired temperature and feed gas was introduced. Its composition was regulated by a five-channel mass flow controller (UNIT Instrument, URS-100) to a desired value. In our standard runs, a typical inlet gas composition was 0.1% NO, 2.0% $O_2$, and 0.1% $NH_3$ or 0.1% isobutane, balanced with ultrahigh-purity helium. The total flow rate was accurately maintained at 300 ± 1.0 mL/min. When desired, 10% $H_2O$ was added by passing the $O_2$/He flow at a constant rate through a water saturator maintained at 80 ± 0.2°C. To avoid condensation of water, the whole line was wrapped with heating tape and kept at 90°C. Before any product analysis, the reactor temperature was kept constant for 30 min. A chemiluminescence NO/$NH_3$ analyzer (Thermo Environmental Instrument, Model 17C) was used for continuous on-line monitoring of the concentrations of NO, $NO_2$, and $NH_3$, while $N_2$, $N_2O$, CO, and $CO_2$ were analyzed by an on-line GC-TCD (HP 5890) with Alltech 13X molecular sieve and Poropak Q columns. Conversions were calculated by

$$\mathrm{Conv}_{NO}(\%) = 100\% \times \left(C_{NO}^{inlet} - C_{NO}^{outlet}\right)/C_{NO}^{inlet} \quad [5a]$$

$$\mathrm{Conv}_{NH_3}(\%) = 100\% \times \left(C_{NH_3}^{inlet} - C_{NH_3}^{outlet}\right)/C_{NH_3}^{inlet}. \quad [5b]$$

From the sum of all N compounds (NO, $NO_2$, $N_2O$, $N_2$, and $NH_3$) at the reactor inlet and outlet, the nitrogen mass balance was checked and found to be >96%. With isobutane as reductant, only GC-TCD was used to analyze the products, and the conversion of NO was determined from the formation of $N_2$. The isobutane conversion was calculated from the amounts of CO and $CO_2$ in the effluent.

### 2.3. *Isotopic Labeling*

Isotopic $^{15}NO$ (provided by Matheson, purity ≥99%) was used in runs at 140 Torr in a recirculating manifold equipped with a Dycor quadrupole gas analyzer. The catalyst, 0.4 g of Fe/MFI, was charged in a Pyrex U-shaped reactor with a bypass valve. The volume of the circulation loop is 145 mL when the reactor is bypassed, but 166 mL when the reactor is open. An electromagnetic-driven gas circulation pump was installed inside the loop to mix the reactants and enforce gas circulation through the catalyst bed with a flow rate of 100 mL/min. After evacuation for 30 min or when the background pressure was below $10^{-3}$ Torr, a gas mixture of typically (i) 20 Torr $NH_3$ + 80 Torr Ar for $NH_3$ adsorption, or (ii) 20 Torr $^{15}NO$ + 20 Torr Ar + 100 Torr $O_2$ for SCR reaction, was admitted into the circulation loop with the reactor being bypassed. After mixing for 1 h the gas mixture was circulated over the catalyst at the desired temperature for 100 min. To correct for the pressure change due to volume expansion, all signal intensities were normalized using the $Ar^+$ peak ($m/e = 40$) as an internal standard.

### 2.4. *Temperature-Programmed Reaction (TPR)*

TPR profiles were usually registered in flowing He (flow rate, 60 mL/min) and recorded on a TP-mass spectrometer attached to the Dycor quadrupole gas analyzer system. The mass spectrometer with 12 channels can monitor all products simultaneously. For coadsorption on Fe/MFI, a feed of $^{15}NO + NH_3 + O_2$ was used, followed by flushing with UHP He (99.995%, further purified over a 4 Å molecular sieve and $MnO/SiO_2$ traps) for 30 min until a stable baseline was established. TPR profiles were registered in the same flow while the temperature was increased from room temperature to 600°C at 8°C/min.

### 2.5. *FTIR Spectra*

A Nicolet 60SX FTIR spectrometer equipped with a liquid nitrogen-cooled MCT detector was used to monitor adsorption and desorption of NO and $NO + O_2$ at room temperature and to produce the IR spectra of the adsorbed groups at constant or variable temperature. The spectral resolution is 1 $cm^{-1}$ (typically 64 scans). Fe/MFI samples were pressed into self-supporting wafers of 8–10 mg/$cm^2$ and placed into a Pyrex glass cell sealed with NaCl windows. The samples were calcined *in situ* to 450°C in a 10% $O_2$-in-He flow of 100 mL/min, followed by cooling to the desired temperature. To follow adsorption, a flow of 0.5% NO + He or 0.5% NO + 2% $O_2$ + He was passed through the cell at a total flow rate of 100 mL/min; the spectra were recorded simultaneously. When desorption or reaction at different temperatures was monitored, the spectrum of Fe/MFI in the He flow, taken at the same temperatures, was used as a reference and subtracted from the corresponding spectrum. When desired, the temperature was raised at a rate of 2°C/min under continuously flowing gases (NO + He or NO + $O_2$ + He) and kept at the desired temperature for 10 min while the IR spectrum was recorded.

## 3. RESULTS

### 3.1. *Activity of Fe/MFI for the SCR Using Ammonia or Isobutane as a Reductant*

The SCR performance of Fe/MFI was tested with ammonia or isobutane as the reductant under identical conditions, both with and without water in the feed. As the reaction rate is much higher with ammonia than with isobutane, a higher space velocity ($3.6 \times 10^5$ $h^{-1}$) was used in these tests than in our previous work. As a consequence, the activity profile with isobutane has a lower $N_2$ yield maximum and it appears at a 50°C higher temperature than in our previous tests with a GHSV of $4.2 \times 10^4$ $h^{-1}$. With the high space velocity, water in the feed is found to promote the $NO_x$ reduction with isobutane over the entire temperature range. As found earlier, the $CO/CO_2$ ratio is higher with the wet than with the dry feed (10).

Figures 1 and 2 show the reduction profiles. Clearly, ammonia reduces $NO_x$ much faster than isobutane does. In the absence of water, the conversion is ∼30% for both NO and $NH_3$ even at 200°C. At 300°C, the NO conversion exceeds 80% with ammonia, but reaches only 17% with iso-$C_4H_{10}$. The maximum NO conversion of ∼90% is reached at about 350°C; it remains high over a wide temperature range, but decreases when $NH_3$ oxidation to NO becomes detectable. The maximum depends on the amount of ammonia available in the feed. With 15% excess of $NH_3$, the conversion of NO is 100%. Interestingly, $NO_2$ becomes detectable only after ammonia is totally consumed. The ammonia consumption increases more steeply with temperature than that of NO; however, the consumption ratio below 450°C remains >0.8. It does not change when $NO_2$ is detectable. Remarkably, the consumption ratio is always higher than 0.75. This finding argues against reaction [2] as the dominant chemistry of the SCR of NO with $NH_3$ over Fe/MFI.

The effect of water on NO conversion is very different with ammonia and isobutane. As shown in Fig. 1B, the

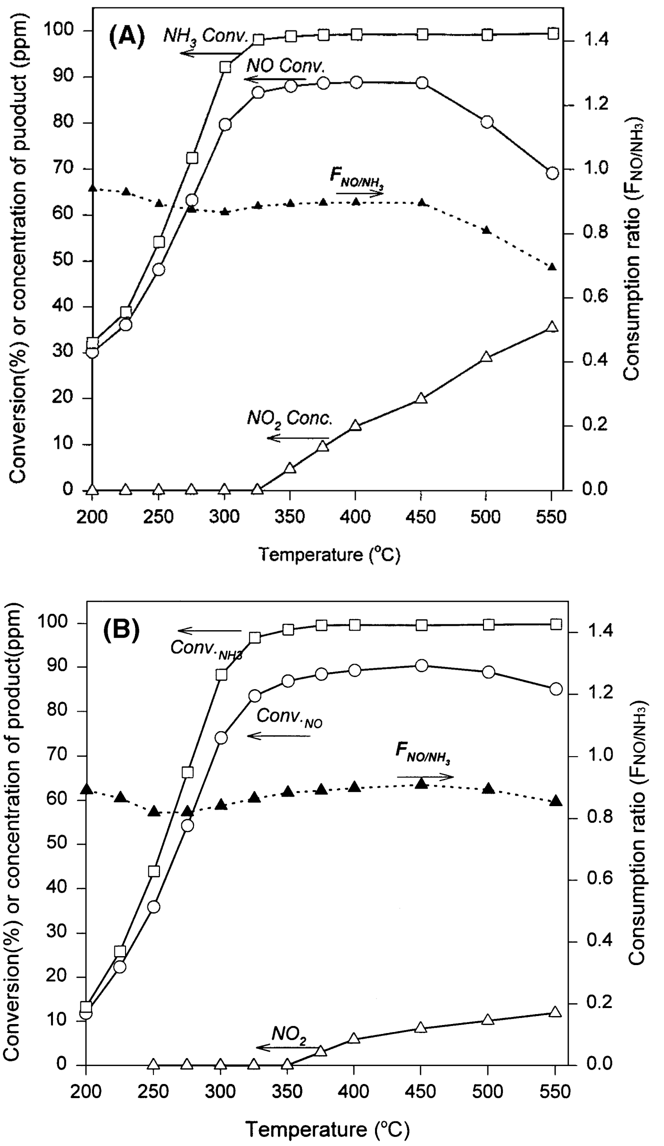

**FIG. 1.** Selective reduction of $NO_x$ with ammonia in dry feed (A) and in 10% $H_2O$ (B) over Fe/MFI catalyst prepared by sublimation of $FeCl_3$. NO, 0.1%; $NH_3$, 0.1%; $O_2$, 2.0%. GHSV $= 3.6 \times 10^5$ $h^{-1}$. (○) NO conversion with dry feed; (△) iso-$C_4H_{10}$ to CO with dry feed; (▽) iso-$C_4H_{10}$ to $CO_2$ with dry feed; (●) NO conversion with 10% $H_2O$ feed; (▲) iso-$C_4H_{10}$ to CO with 10% $H_2O$ feed; (▼) iso-$C_4H_{10}$ to CO with 10% $H_2O$ feed.

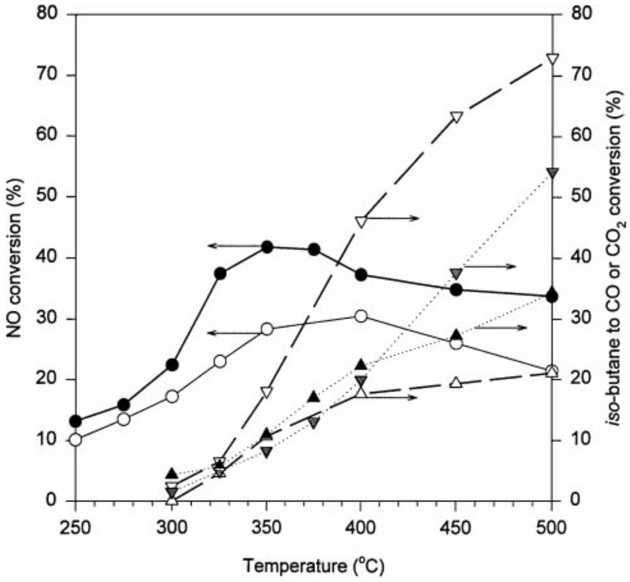

**FIG. 2.** Selective reduction of $NO_x$ with isobutane in dry feed and 10% $H_2O$ over Fe/MFI catalyst prepared by sublimation of $FeCl_3$. NO, 0.1%; isobutane, 0.1%; $O_2$, 2.0%. GHSV $= 3.6 \times 10^5$ $h^{-1}$.

NO conversion over Fe/MFI is significantly suppressed at low temperature, without, however, changing the value of the maximum NO conversion. At high temperature water vapor seems to suppress ammonia oxidation to NO, so that the temperature window of high NO conversion becomes wider. Less $NO_2$ is found with the wet than the dry feed. The consumption ratio of $NH_3$ to NO is little affected by the addition of water and it remains high even at high temperature.

The hydrothermal stability of the Fe/MFI catalyst under the conditions of $NO_x$ reduction with $NH_3$ is illustrated by a 100 h test at 350–400°C with several switches between a dry and a wet feed. The result in Fig. 3 shows that such multiple switches do not affect the conversion of NO and $NH_3$. At the end of this test the conversion of $NH_3$ is still 100%. Since acid sites are neutralized by ammonia not much dealumination is expected to take place in more extended tests. The absence of a negative effect of water on the activity and

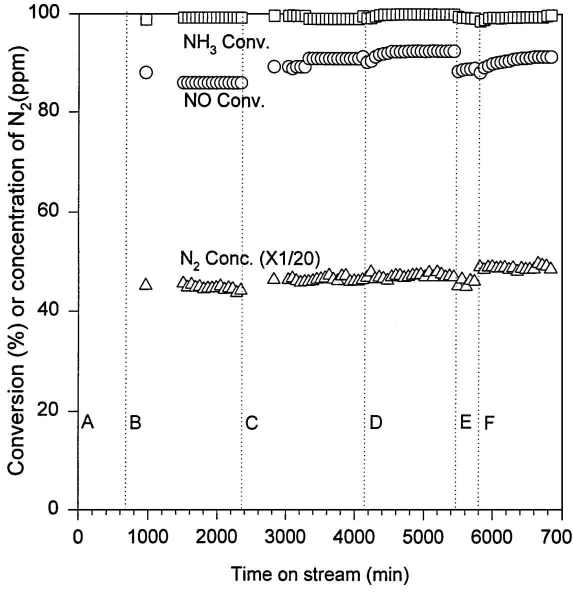

**FIG. 3.** Durability of Fe/MFI catalyst for SCR of $NO_x$. (A) Initial process, (B) dry feed at 350°C, (C) 10% $H_2O$ feed at 400°C, (D) dry feed at 400°C, (E) dry feed at 350°C, (F) 10% $H_2O$ feed at 400°C. NO, 0.1%; $NH_3$, 0.1%; $O_2$, 2.0%, GHSV $= 3.6 \times 10^5$ $h^{-1}$.

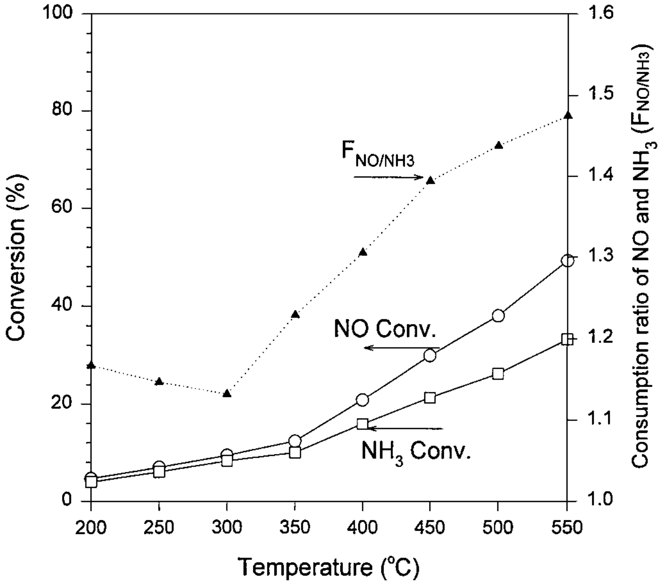

**FIG. 4.** Reduction of NO with $NH_3$ in $O_2$-free feed at different temperatures over Fe/MFI catalyst prepared by the sublimation method. NO, 0.1%; $NH_3$, 0.1%, GHSV $= 3.6 \times 10^5\ h^{-1}$.

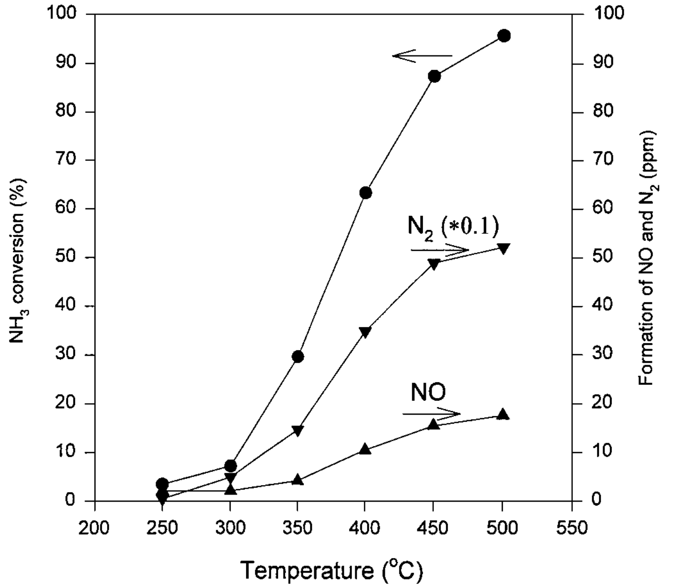

**FIG. 5.** $NH_3$ oxidation over Fe/ZSM-5 catalyst. $NH_3$, 0.1%; $O_2$, 2.0%. GHSV $= 4.5 \times 10^5\ h^{-1}$.

durability of Fe/MFI catalysts is in agreement with results of Ma and Grünert (28) and previous work with alkane reduction by Feng and Hall (32) and our group (10).

Dioxygen in the feed was found to enhance the reaction substantially. As shown in Fig. 4, the reaction of $NO + NH_3$ is very slow with an oxygen-free feed: only 10% NO is converted at 350°C. Even at 550°C, the NO conversion is below 50%. It follows that the rate of reaction [1] is very low or zero. We cannot exclude that the low observed NO conversion in Fig. 4 is due to the disproportionation of NO to $N_2O + NO_2$ that was previously detected over MFI-supported Cu and Fe catalysts (22, 33), followed by reduction of these products. We shall therefore disregard reaction [1] as a significant contributor to $NO_x$ reduction in $O_2$-containing feeds.

The oxidation of ammonia with a large excess of $O_2$ in an NO-free feed is shown in Fig. 5. The ammonia conversion is 34% at 360°C and 90% at 460°C. The selectivity is 98% to $N_2$ and 2% to NO. Comparison with Fig. 1 shows that ammonia reacts much faster with $NO_x$ than with $O_2$ even if the latter is present in very large excess. This confirms that the present Fe/MFI catalyst is not only very active, but also highly selective for the SCR of $NO_x$ with $NH_3$.

### *3.2. Identification of Reaction Mechanism by Isotopic Labeling*

Analysis of the product of $^{15}N$-labeled $NO_x$ conversion with adsorbed $^{14}NH_3$ provides an important clue for the reaction mechanism. Fe/MFI, which was precalcined at 500°C in a pure $O_2$ flow, was exposed at room temperature for 1 h to a circulating gas mixture of 20 Torr $NH_3$ and 80 Torr Ar, followed by evacuation for 30 min. This sample was subsequently exposed to a circulating mixture of 20 Torr $^{15}NO$, 20 Torr Ar, and 100 Torr $O_2$. Figure 6 shows the normalized 12 signal intensities of $^{15}N^{14}N$ ($m/e = 29$), $^{14}N_2$ ($m/e = 28$), $^{14}N_2O$ ($m/e = 44$), and $^{15}N^{14}NO$ ($m/e = 45$) in the products, plotted against reaction time. Clearly, $^{15}N^{14}N$ is the dominant product; its signal intensity increases steeply, and reaches >90% within 30 min. Evidently, one of the N atoms

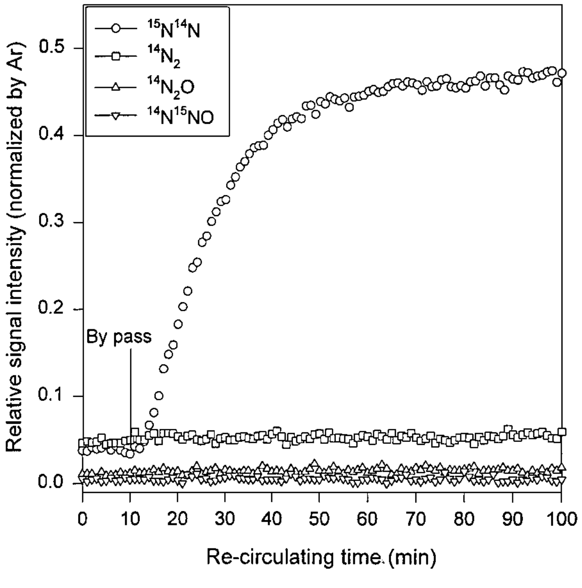

**FIG. 6.** Time dependence of the relative signal intensity upon cirulating a mixture of 20 Torr $^{15}NO$ + 20 Torr Ar + 100 Torr $O_2$ over $^{14}NH_3$ pre-adsorbed Fe/MFI at room temperature.

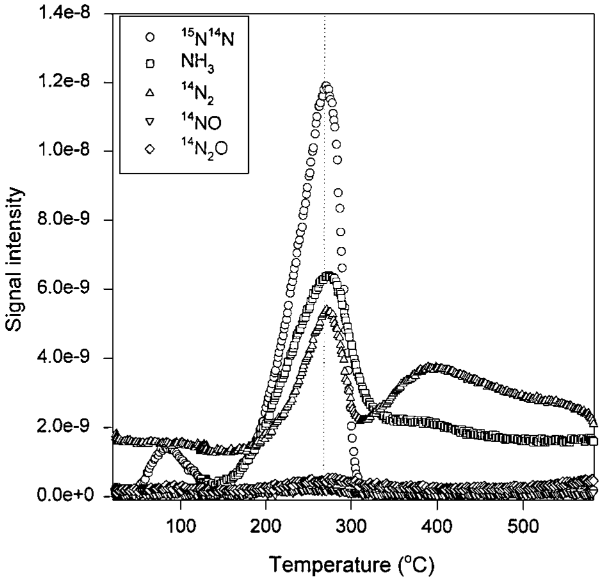

**FIG. 7.** Temperature-programmed desorption after circulating for 100 min, followed by evacuation for 30 min.

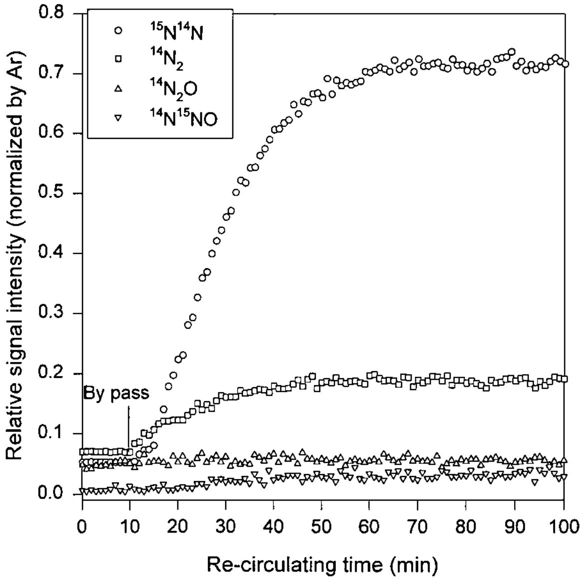

**FIG. 8.** Time dependence of the relative signal intensity upon circulating a mixture of 20 Torr $^{15}NO$ + 20 Torr Ar + 100 Torr $O_2$ over $^{14}NH_3$ pre-adsorbed Fe/MFI at 280°C.

in the $N_2$ product comes from $^{15}NO$, the other from $^{14}NH_3$. Oxidation of $^{14}NH_3$ with $O_2$ to $^{14}N_2$ is negligible at this temperature.

After the gas was circulated for 100 min, followed by evacuation for 30 min, the adsorbates were released by increasing the temperature with a ramp of 8°C/min. As shown in Fig. 7, one $^{15}N^{14}N$ peak appears at 85°C and a family of peaks at 280°C, which contain the masses of $m/e = 29$ for $^{15}N^{14}N$, $m/e = 28$ for $^{14}N_2$, and $m/e = 17$ for $^{14}NH_3$. Weak signals with $m/e = 46$ attributed to $^{14}N_2O$ and a trace of $m/e = 30$ for $^{14}NO$ also appear at this temperature. The intensity ratio of $^{15}N^{14}N$ and $^{14}N_2$ is about 2/1. The fact that these peaks are formed at the same temperature suggests that they are produced in a concerted reaction. The $m/e = 29$ peaks at 85°C and 280°C indicate reaction of adsorbed $^{15}NO_x$ with two forms of adsorbed $^{14}NH_3$, one of which might be $NH_4$ ions.

Figure 8 shows a test at 280°C with a mixture of $^{15}NO$ and an excess of $O_2$ circulating over a catalyst carrying preadsorbed $^{14}NH_3$. Again, $^{14}N^{15}N$ is the predominant $N_2$ product, but non-negligible formation of $^{14}N_2$ is also noted; the ratio of the isotopomers is found to be $^{15}N^{14}N/^{14}N_2 = 5.5$.

As the consumption ratio of 1/1 indicates that reactions of the type [3] dominate in the $NO_x$ reduction with ammonia, it might be expected that reduction of a labeled mixture of $NO/NO_2 = 1/1$ with unlabeled $NH_3$ will yield pure $^{15}N^{14}N$. To check this, a mixture with this $NO/NO_2$ ratio has been prepared by dosing 20 Torr $^{15}NO$ and 5 Torr $O_2$, making use of the fact that the gas-phase equilibrium,

$$2NO + O_2 \rightleftharpoons 2NO_2, \qquad [6]$$

at room temperature with a huge equilibrium constant ($K^\circ_{298} = 2.4 \times 10^{12}\ \mathrm{Pa}^{-1}$) is established within minutes even in the absence of a catalyst, as is evidenced by the color change. The gas mixture was stored for 1 h in the bypass tube before being circulated over the $NH_3$-covered catalysts at room temperature. The conditions were further the same as for the run in Fig. 6. The result, in Fig. 9, clearly

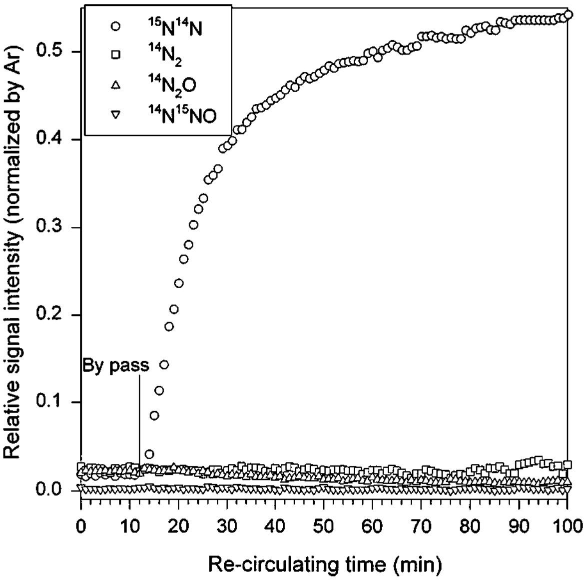

**FIG. 9.** Time dependence of the relative signal intensity upon circulating a mixture of 20 Torr $^{15}NO$ + 20 Torr Ar + 5 Torr $O_2$ + 100 Torr He over $^{14}NH_3$ pre-adsorbed Fe/MFI at room temperature.

shows a high production of extremely pure $^{14}N^{15}N$ (the normalized intensity of $m/e = 29$ by $Ar^+$ is larger than or at least equal to that in Fig. 6), proving that it is *not* necessary to convert all NO into $NO_2$, but that the 1/1 mixture which is equivalent to $N_2O_3$ suffices to attain maximum conversion with adsorbed ammonia.

Trace amounts of $^{14}N_2$ ($m/e = 28$) and $^{14}N_2O$ ($m/e = 44$) in this run do not change with reaction time, indicating that they are background signals, not by-products.

### 3.3. *IR Spectroscopy of Adsorption Complexes of the Type $NO_y$ ($y > 1$)*

*3.3.1. NO adsorption/desorption.* IR spectra of NO adsorption on a calcined Fe/MFI catalyst at room temperature are in agreement with our previous work (34) and literature results (35–37). Three major bands at 2133, 1879, and 1809 $cm^{-1}$, with shoulders at 1918, 1858, and 1779 $cm^{-1}$, are assigned to (a) $NO^+$ ions at cation-exchange sites of MFI, (b) [Fe(NO)] complexes with Fe ions located at different exchange sites (1879 and 1858 $cm^{-1}$), and (c) Fe dinitrosyl groups, $[Fe(NO)_2)]$ with Fe ions in accessible positions (1918 and 1809 $cm^{-1}$), respectively (34, 37). The bands at 2133, 1879, 1858, and 1809 $cm^{-1}$ are quickly formed upon exposure to NO + He; no obvious change was observed with longer exposure times. However, upon flushing with He, the intensity of the 2133 and 1809 $cm^{-1}$ bands decreases, while that of the 1620 and 1578 $cm^{-1}$ bands, attributed to $NO_y$ groups, increases. Upon increasing temperature in He flow, the bands at 2133 and 1809 $cm^{-1}$ quickly disappear, while the 1879 $cm^{-1}$ band decreases gradually without, however, vanishing even at 400°C. In concert with this, a fast increase of the bands at 1620 and 1579 $cm^{-1}$ is observed. This could indicate that $NO_y$ groups are formed by oxidation of adsorbed NO with structural oxygen of the Fe/MFI catalyst.

IR spectra, recorded during the temperature increase in 0.5% NO + He flow, are shown in Fig. 10. The 2133 $cm^{-1}$ band decreases very slowly and remains detectable at 240°C. The 1879 $cm^{-1}$ band decreases gradually, while the 1620 $cm^{-1}$ ($NO_2$) and 1579 $cm^{-1}$ ($NO_3^-$) bands increase below 80°C, but decrease upon further raising the temperature. Their intensities are much weaker than in flowing He. The 1879 $cm^{-1}$ band persists strongly at 400°C, while the 1620 and 1579 $cm^{-1}$ bands disappear above 240°C.

*3.3.2. $NO + O_2$ adsorption/desorption.* Figure 11 shows the IR spectra of adsorption complexes at different times of exposure to a flow of 0.5% NO + 2.0% $O_2$. They strongly differ from those observed in the absence of $O_2$. A band at 2133 $cm^{-1}$, ascribed to $NO^+$, reaches a maximum within 2 min, and then decreases gradually with increasing exposure time, while another band at 2185 $cm^{-1}$ develops. Although the intensity ratio of the 2185 and 2133 $cm^{-1}$ bands increases, their total intensities decrease to a very low level during exposure to NO + $O_2$ for 30 min. The band at 1876 $cm^{-1}$ is ascribed to a superposition of two adsorbed groups, NO and $N_2O_3$. The 1745 $cm^{-1}$ band might be due to the dimer of nitrogen dioxide ($N_2O_4$) (38). The 2185 $cm^{-1}$ band has been assigned to a complex of $NO^+$ with $[N_2O_4]$ (36). $N_2O_3$ produces not only the band at 1879 $cm^{-1}$ but also a band at 1578 $cm^{-1}$, which overlaps with the band of nitrate ion, and a band at 1297 $cm^{-1}$. $N_2O_3$, NO, and $N_2O_4$

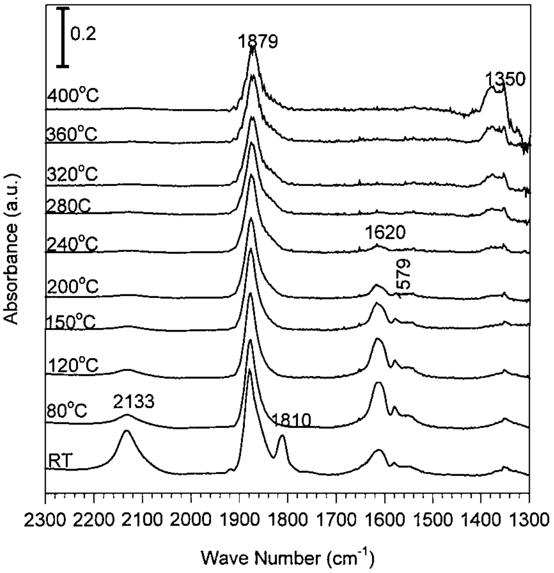

**FIG. 10.** FTIR spectra of NO adsorbed on Fe/MFI catalyst, taken during temperature-programmed process in 0.5% NO + He flow.

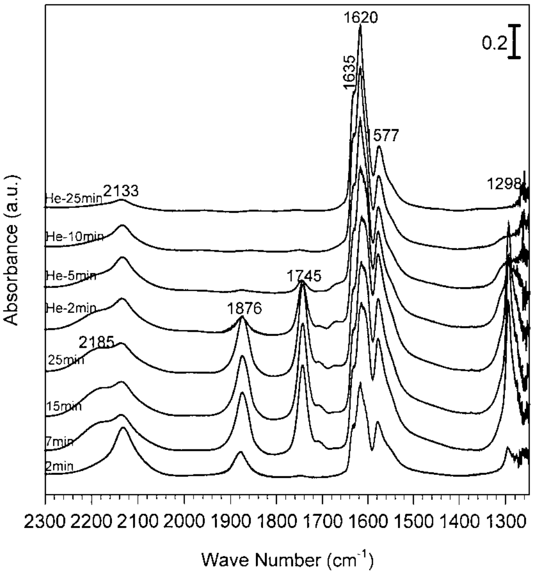

**FIG. 11.** FTIR spectra taken at room temperature of $NO_y$ adsorbed on Fe/MFI catalyst under a flow of 0.5% NO + 2.0% $O_2$ + He at different times and followed by purge with He.

are removed upon flushing with He, while only the nitro group ($NO_2$) and the nitrate ion survive.

The spectra taken in an NO + $O_2$ flow while the temperature is increasing are very different from those taken in He. As shown in Fig. 12, all the adsorbate bands observed in Fig. 11 appear at room temperature, but the bands at 2185, 1746, 1297, and 1880 $cm^{-1}$ attenuate rapidly when the temperature is raised, while the band at 2133 $cm^{-1}$ persists. The band at 1879 $cm^{-1}$, ascribed to an overlap of NO and $N_2O_3$, first decreases steeply but then increases again at higher temperature. We attribute the decrease to the disappearance of adsorbed $N_2O_3$ and the increase to the formation of mononitrosyl. The concentration of that group reaches a maximum at about 360°C. The bands at 2133, 1635, 1620, and 1578 $cm^{-1}$ decrease monotonically, while the 1620 and 1578 $cm^{-1}$ bands are only half as strong as in He flow. A new broad feature emerges at 1352–1420 $cm^{-1}$. It was also observed when the temperature is increased under flowing NO (Fig. 10), but not in flowing He. It might be assigned to a monodentate nitrito or a bridging monodentate nitrito group (39, 40). Apparently, it is due to a rather stable adsorption complex on Fe/MFI.

The IR results reveal that NO and $NO_2$ are competitively adsorbed at the same sites at various temperatures. Their relative concentrations on the surface depend on the gas-phase composition and the temperature. Under our typical reaction conditions, adsorbed NO, $NO_2$, nitrate, and nitrite groups will coexist on the catalyst.

*3.3.3. Effect of $H_2O$ on the formation of adsorption complexes.* Figure 13 compares the adsorption complexes on Fe/MFI after calcination and exposure to $H_2O$. Clearly, there are striking differences. The strong bands at 2185, 2133, 1735, and 1620 $cm^{-1}$ observed on the clean catalyst are not detected in the presence of adsorbed $H_2O$. The bands at 1876 $cm^{-1}$ (NO and $N_2O_3$), 1298 $cm^{-1}$ ($N_2O_3$), and 1745 $cm^{-1}$ ($N_2O_4$) are very weak. A strong peak at 1309 $cm^{-1}$ can be attributed to a nitro group ($NO_2$). While they are formed a strong negative peak appears at 1630 $cm^{-1}$ and gets stronger, indicating that water is expelled by $NO_2$ from the catalyst surface. It follows that the $NO_y$ groups and $H_2O$ compete for the same adsorption sites. If the water pressure in the gas phase is low, the $NO_y$ groups will prevail on these sites. When nitrite ions coexist with adsorbed water, a band appears at 1394 $cm^{-1}$. A peak at 1601 $cm^{-1}$ could be due to $NO_2$ that is weakly adsorbed on ferric oxide nanoclusters, but in view of the strong negative peak at 1630 $cm^{-1}$, we prefer to attribute it to a combination of adsorbed $NO_2$ (1620 $cm^{-1}$) and the negative peak (1630 $cm^{-1}$). Almost no NO band was observed in the presence of water, indicating that the former adsorption is much weaker than that of $H_2O$. Figure 13c confirms that NO is unable to displace adsorbed $H_2O$ from the surface; almost no NO adsorption is detected. Only a weak peak at 1847 $cm^{-1}$ might be due to interaction between NO and $Fe^{3+}$ ions that are carrying $H_2O$ ligands.

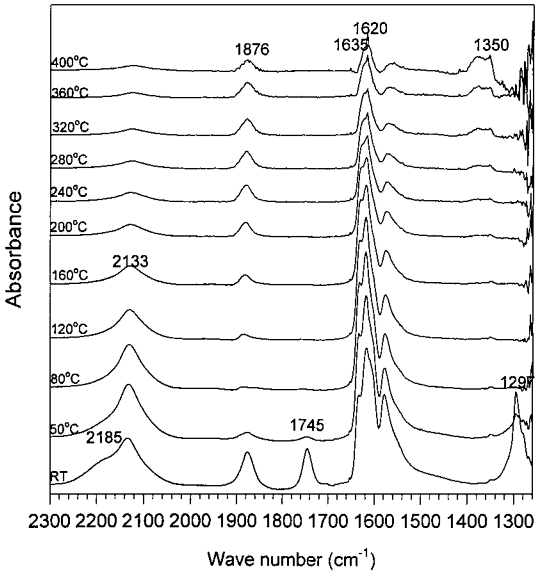

**FIG. 12.** FTIR spectra of $NO_y$ adsorbed on Fe/MFI catalyst, taken during a temperature-programmed process in 0.5% NO + 2.0% $O_2$ + He flow.

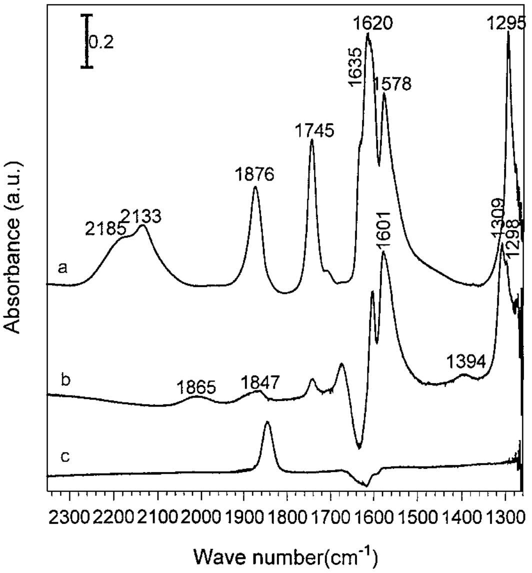

**FIG. 13.** FTIR spectra taken at 7 min of $NO_y$ on (a) calcined Fe/MFI under a flow of 0.5% NO + 2.0% $O_2$ + He, (b) $H_2O$ pre-adsorbed Fe/MFI under a flow 0.5% NO + 2.0% $O_2$ + He, and (c) $H_2O$ pre-adsorbed Fe/MFI under a flow of 0.5% NO + He at room temperature.

## 4. DISCUSSION

A number of hitherto open questions can be answered on the basis of the data in this paper and some insight has been gained on the complexes that populate the catalytically active sites during $NO_x$ reduction.

**TABLE 1**

**SCR Catalytic Performance of Various Catalysts at Low Temperature**

| Sample | $T$/°C | NO conv/% | Specific activity $\times 10^6$/mol · g$^{-1}$ · s$^{-1}$ | TON[e] $\times 10^3$/s$^{-1}$ |
|---|---|---|---|---|
| Fe/MFI[a] | 200 | 30 | 2.7 | 4.5 |
| | 225 | 36 | 3.2 | 5.4 |
| | 250 | 48 | 4.3 | 7.5 |
| | 275 | 62 | 5.6 | 10.1 |
| | 300 | 80 | 7.1 | 12.8 |
| Fe/MFI[b] | 250 | 22 | 1.2 | — |
| | 300 | 60 | 3.3 | — |
| Fe/MFI[c] | 250 | 9 | 0.7 | 2.4 |
| | 300 | 27 | 2.0 | 7.1 |
| Cu/MFI[d] | 250 | 5 | 0.2 | — |
| | 300 | 20 | 1.1 | — |

[a] Prepared by sublimation process in this work. Reaction conditions: 25 mg of catalyst; total flow, 300 mL · min$^{-1}$ with composition of 0.1% NO, 0.1% $NH_3$, 2.0% $O_2$ balanced by He.

[b] Prepared by modified sublimation process in Ref. (28). Reaction conditions: 35 mg of catalyst; total flow, 260 mL · min$^{-1}$ with composition of 0.1% NO, 0.1% $NH_3$, 2.0% $O_2$ balanced by He.

[c] Prepared by ion-exchange process in Ref. (30). Reaction conditions: 50 mg of catalyst; total flow, 500 ml/min with composition of 0.1% NO, 0.1% $NH_3$, 2.0% $O_2$ balanced by He.

[d] Prepared by ion-exchange process in Ref. (29). Reaction conditions: GHSV $= 3.03 \times 10^5$ mL · g$^{-1}$ · h$^{-1}$; gas composition, 0.1% NO, 0.1% $NH_3$, 2.0% $O_2$ balanced by He.

[e] Number of converted NO molecules per iron per second.

First, it is obvious that under identical conditions ammonia is a much more effective reductant in the SCR than isobutane. At a very high space velocity NO conversion to $N_2$ reaches only 30% with isobutane, but 100% of NO is reduced to $N_2$ with ammonia if present in a small excess. If ammonia and nitrogen oxide are dosed in a 1/1 ratio, the NO conversion reaches 90% at 100% $NH_3$ conversion. Compared with the data reported in the literature on Cu/MFI (24) or Fe/MFI prepared by wet ion exchange (29), the catalytic activity of the present catalyst is much higher, notably at low temperatures. As shown in Table 1, Fe/MFI prepared by sublimation gives 48% NO conversion at 250°C, while ion-exchanged Fe/MFI and Cu/MFI only give 5% and 9% NO conversion, respectively. The higher turnover frequency of the present catalysts is believed to be due to the high iron loading. At high temperatures some ammonia oxidation is unavoidable over this catalyst as it is over Cu/MFI, HMFI (24, 41, 42), and Fe/MFI catalysts prepared by a modified sublimation method (28). Still, the data in Figs. 1 and 5 indicate a very high selectivity of Fe/MFI for $NO_x$ reduction.

For the SCR of $NO_x$ with isobutane over Fe/MFI (15) it was previously proposed that an adsorbed intermediate is formed that rearranges to a complex displaying amine-like groups which react with $NO + O_2$ to form $N_2$. The present work shows the mechanistic commonality of $NO_x$ reduction with hydrocarbons and ammonia over this family of catalysts. With ammonia the difficult rearrangement steps can be bypassed that are responsible for the lower efficiency of the SCR with hydrocarbons; this results in superior efficiency.

The present results also rationalize the finding that water lowers the conversion at low temperature because it competes with the reactants for the active sites. At high temperature, when many sites are bare, this competition is kinetically irrelevant, but the role of water in the formation of ammonium nitrite can become relevant, as will be shown below. This is fundamentally different from the situation encountered when hydrocarbons are used to reduce NO. In that case deposits are formed that tend to block the sites required for NO oxidation. Water helps to volatilize such deposits, thus increasing catalytic activity. Moreover, water can help in the conversion of nitriles to amines. Water vapor therefore promotes activity of SCR with hydrocarbons at temperatures below ~300°C

We find no support for the claim of some authors (31) that water could act by enhancing the acidity of zeolite-based catalysts. On the contrary, the acid sites are neutralized by adsorption of ammonia. Literature data also show that on zeolite-based catalysts, such as Cu/MFI or HMFI, the SCR reaction is of zero or negative order in ammonia (24, 41, 43). This shows that stronger acidity would not do any good; it rather suggests that the active sites are highly covered with ammonia under typical SCR reaction conditions.

New insights on the reaction mechanism of $NO_x$ reduction with $NH_3$ are obtained by the combination of FTIR data with a careful analysis of the $NO/NH_3$ consumption ratio and the work with isotopically labeled molecules. In order to evaluate the analysis of the nitrogen isotopomers it is useful to rewrite the equations of the hypothetical reactions [1]–[3] for the scenario where the nitrogen oxide in the feed is $^{15}NO$, but ammonia is $^{14}NH_3$. We assume that $N_2O_3$ will always be in equilibrium with $NO + NO_2$, but we will write [3a′] for the anhydrous oxide and [3b′] for its presence as ammonium nitrite:

$$3\,{}^{15}\mathrm{NO} + 2\,{}^{14}\mathrm{NH_3} \rightarrow 2\,{}^{14}\mathrm{N}{}^{15}\mathrm{N} + 0.5\,{}^{15}\mathrm{N_2} + 3\mathrm{H_2O} \qquad [1']$$

$$3\,{}^{15}\mathrm{NO_2} + 4\,{}^{14}\mathrm{NH_3} \rightarrow 3\,{}^{14}\mathrm{N}{}^{15}\mathrm{N} + 0.5\,{}^{14}\mathrm{N_2} + 6\mathrm{H_2O} \qquad [2']$$

$${}^{15}\mathrm{N_2O_3} + 2\,{}^{14}\mathrm{NH_3} \rightarrow 2\,{}^{14}\mathrm{N}{}^{15}\mathrm{N} + 3\,\mathrm{H_2O} \qquad [3a']$$

$$\mathrm{H}{}^{15}\mathrm{NO_2} + {}^{14}\mathrm{NH_3} \rightleftharpoons {}^{14}\mathrm{NH_4}{}^{16}\mathrm{NO_2} \Rightarrow {}^{14}\mathrm{N}{}^{15}\mathrm{N} + 2\mathrm{H_2O}. \qquad [3b']$$

The present results clearly show that neither [1] nor [2] describes the mechanism correctly; both the consumption ratio at low temperature and the predominant formation of $^{14}N^{15}N$ show that only Eqs. [3a′] and [3b′] are in agreement with experimental facts. Figure 6 clearly shows that at low temperature $^{14}N^{15}N$ is the only detectable $N_2$ isotopomer.

At this temperature the concentrations of $NH_3$ and $H_2O$ in the adsorbed layer are favorable for the formation of ammonium nitrite.

Additionally, the isotopic data of the TPR experiment of Fig. 7 are easily rationalized with this mechanism. In that run the catalyst surface is most likely populated with adsorbed ammonia and binuclear iron oxo-ions that have exchanged their $OH^-$ groups with $NO_3^-$ groups. Irrespective of the actual sequence of events, one can distinguish chemical reduction steps leading to $^{14}N_2$ and steps in which ammonia reacts with nitrite groups to form $^{14}N^{15}N$. The former group of reactions are given by.

$$\begin{aligned}&\left[{}^{15}NO_3\text{–Fe–O–Fe–}{}^{15}NO_3\right]^{2+} + 2\,{}^{14}NH_3\\ &\quad\rightarrow \left[{}^{15}NO_2\text{–Fe–}\square\text{–Fe–}{}^{15}NO_2\right]^{2+} + {}^{14}N_2 + 3H_2O,\end{aligned} \qquad [7]$$

but the reaction of $^{14}NH_3$ with the nitrite ions, $^{15}NO_2^-$, will produce $^{14}N^{15}N$, and the water will provide the OH groups replacing the nitrite ligands:

$$\begin{aligned}&\left[{}^{15}NO_2\text{–Fe–}\square\text{–Fe–}{}^{15}NO_2\right]^{2+} + 2\,{}^{14}NH_3\\ &\quad\rightarrow [HO\text{–Fe–}\square\text{–Fe–}OH]^{2+} + 2\,{}^{14}N^{15}N + 2H_2O.\end{aligned} \qquad [8]$$

The overall process thus becomes

$$\begin{aligned}&\left[{}^{15}NO_3\text{–Fe–O–Fe–}{}^{15}NO_3\right]^{2+} + 4\,{}^{14}NH_3\\ &\quad\rightarrow [HO\text{–Fe–}\square\text{–Fe–}OH]^{2+} + {}^{14}N_2\\ &\qquad + 2\,{}^{14}N^{15}N + 5H_2O,\end{aligned} \qquad [9]$$

with a ratio of the isotopomers equal to $^{14}N^{15}N/^{14}N_2 = 2/1$. This ratio is indeed equal to the ratio found in Fig. 7 for the $N_2$ isotopomers desorbed at 280°C.

The result of the run at 280°C in Fig. 8 is also consistent with the new model. In this run $^{15}NO$ was first oxidized with $O_2$ to $^{15}NO_2$. When interacting with ammonia this gas will be reduced to the 1/1 ratio of NO and $NO_2$, equivalent to $^{15}N_2O_3$, in a process oxidizing $^{14}NH_3$ to $^{14}N_2$. The $^{15}N_2O_3$ equivalent oxide will further be reduced by $^{14}NH_3$ according to [3b′]. Summing this up, one obtains

$$6\,{}^{15}NO_2 + 8\,{}^{14}NH_3 \rightarrow {}^{14}N_2 + 6\,{}^{14}N^{15}N + 12H_2O, \qquad [10]$$

with a ratio $^{14}N^{15}N/^{14}N_2 = 6$. This is close to the observed ratio of 5.5 in Fig. 8. The difference might be due to some reduction of bridging oxygen with ammonia, producing additional $^{14}N_2$.

Another test probing this mechanistic model is shown in Fig. 9. In this case the gas-phase equilibrium of the molecules NO, $NO_2$, and $O_2$ was established at room temperature with a feed containing just enough $O_2$ to oxidize 50% of the NO, in order to establish a ratio of $NO/NO_2 = 1/1$. As Fig. 9 shows, this dosage results in a high reactivity, leading indeed to ~100% $^{14}N^{15}N$.

In summary, the results with labeled $^{15}NO$ show that reduction with ammonia of $N_2O_3$, or an equivalent combination of oxides with nitrogen in an average oxidation state of $N^{3+}$, is the crucial process in the SCR of $NO_x$. As the nitrogen atom in ammonia has the formal oxidation state of $N^{3-}$, the formation of $N_2$ is thus given by

$$N^{3+} + N^{3-} \rightarrow (N^0)_2. \qquad [11]$$

The IR data are in agreement with the above interpretation. They provide direct evidence for the presence of $N_2O_3$ at low temperature in a dry atmosphere. Infrared bands at 1879, 1578, and 1298 $cm^{-1}$ have been ascribed to this oxide. It stands to reason that it will easily decompose at higher temperature, but also that it reacts with water and ammonia to ammonium nitrite. The IR spectrum at high temperature reveals the formation of nitrite ions on the catalyst. Therefore, reaction [3] appears to be a plausible process in which $N_2$ is produced. Formation of pure $N_2$ by decomposition of ammonium nitrite is, of course, an old chemistry textbook experiment.

The water required for the formation of ammonium nitrite is amply provided by the reactions forming $N_2$. At low temperature its steady-state concentration on the zeolite will be high, so that it behaves as a conventional competitor for active sites. At high temperature less adsorbed water will be present in the zeolite cavities; its concentration will, however, be increased by a high partial pressure of water in the feed. This beneficial effect of water on the formation of ammonium nitrite is in agreement with the present observation that the reaction order in added water is positive at high temperature. It could be also possible that water suppresses $NH_3$ oxidation at high temperatures; consequently, its selectivity for $NO_x$ reduction is higher.

At low temperatures $NH_3$, $H_2O$, $NO_2$, NO, and $O_2$ all compete for adsorption sites. Among these $NH_3$ appears most strongly adsorbed; its admission causes a measurable increase in the temperature by ~3°C. The present results show that the heat of adsorption of the gases ranks in the order $NH_3 > NO_2 > H_2O > NO$. At 400°C most water is desorbed but considerable amounts of $NO_2$ are retained.

The high efficiency of this catalyst to reduce NO with ammonia in the presence of $O_2$ leads to an important mechanistic conclusion. If the nitrogen oxide were first oxidized to $NO_2$, before becoming reduced by ammonia, the overall consumption of ammonia would be much higher. The calculated values for the consumption ratio $F = NO/NH_3$ are 0.75 for $NO_2$ and 0.60 for $NO_3^-$ ions as reaction intermediates. Even lower values would be expected if also some oxidation of ammonia with $O_2$ took place. The observed values are well above these numbers. It follows that NO is oxidized only to an oxidation state well below that of $NO_2$ (with $N^{4+}$) or $NO_3^-$ (with $N^{5+}$). Ammonia intercepts this oxidation at the state of $N^{3+}$ and reduces it to $N_2$. If the SCR efficiency for $NO_x$ is expressed in terms of reduction equivalents consumed, the Fe/MFI catalyst, prepared by sublimation, uses ammonia much more efficiently than it can use hydrocarbons.

## 5. CONCLUSIONS

Fe/MFI catalysts that were prepared by the sublimation technique are even more active in reducing $NO_x$ with ammonia than with isobutane. The data with $^{15}$N-labeled NO show that a preferred path for the reduction of $NO_x$ with ammonia is via ammonium nitrite, $NH_4NO_2$, which decomposes to $N_2 + H_2O$. In this mechanism one N atom of the $N_2$ products stems from NO, the other from $NH_3$, and the consumption ratio of NO and $NH_3$ is 1/1. Higher $NH_3$ consumption and formation of $^{14}N_2$ besides the preferred $^{14}N^{15}N$ indicate ammonia oxidation by its reaction with either $O_2$ or a nitrogen oxide containing N atoms in a valence state higher than $N^{3+}$.

## ACKNOWLEDGMENTS

This work was supported by the EMSI program of the National Science Foundation and the U.S. Department of Energy, Office of Science (CHE-9810378), at the Northwestern University Institute for Environmental Catalysis. Financial aid from the Director fo the Chemistry Division, Basic Energy Sciences, U.S. Department of Energy, Grant DE-FGO2-87ER13654, is gratefully acknowledged.

## REFERENCES

1. Boot, H., and Janise, F., *Catal. Today* **21**, 369 (1988).
2. Forzatti, P., and Lietti, L., *Heterogeneous Chem. Rev.* **3**, 33 (1996).
3. Busca, G., Lietti, L., Ramis, G., and Berti, F., *Appl. Catal. B* **18**, 1 (1998).
4. Long, R. Q., and Yang, R. T., *Appl. Catal. B* **24**, 13 (2000).
5. Casagrande, L., Nova, I., Forzatti, P., and Baiker, A., *Appl. Catal. B* **22**, 63 (1999).
6. Iwamoto, M., Yahiro, H., Shundo, S., Yu-U, Y., and Mizuno, N., *Shokubai* **32**, 430 (1990).
7. Centi, G., and Perathoner, S., *Appl. Catal. A* **132**, 179 (1995).
8. Fritz, A., and Pitchon, V., *Appl. Catal. B* **13**, 1 (1997).
9. Feng, X., and Hall, W. K., *Catal. Lett.* **41**, 45 (1996).
10. Chen, H.-Y., and Sachtler, W. M. H., *Catal. Today* **42**, 73 (1998).
11. Voskoboinikov, T. V., Chen, H.-Y., and Sachtler, W. M. H., *Appl. Catal. B* **19**, 279 (1998).
12. Li, Y., and Armor, J. N., *Appl. Catal. B* **1**, L31 (1992).
13. Wichterlová, B., Beran, S., Bednářová, S., Nednamová, K., Dudíková, L., and Jírů, P., *Stud. Surf. Sci. Catal.* **37**, 199 (1988).
14. Wang, X., Chen, H.-Y., and Sachtler, W. M. H., *Appl. Catal. B* **26**, L227 (2000).
15. Chen, H.-Y., Voskoboinikov, T. V., and Sachtler, W. M. H., *Catal. Today* **54**, 483 (1999).
16. Chen, H.-Y., Voskoboinikov, T., and Sachtler, W. M. H., *J. Catal.* **186**, 91 (1999).
17. Mergler, Y. J., van Aalst, A., van Delft, J. and Nieuwenhuys, B. E., *J. Catal.* **161**, 310 (1996).
18. Okuhara, T., Hasada, Y., and Misono, M., *Catal. Today* **35**, 83 (1997).
19. Chafik, T., Kameoka, S., Ukisu, Y., and Miyadera, T., *J. Mol. Catal. A* **136**, 203 (1998).
20. Cant, N. W., and Cowan, A. D., *Catal. Today* **35**, 89 (1997).
21. Lobree, L. J., Hwang, I. C., Reimer, J. A., and Bell, A. T., *Catal. Lett.* **63**, 233 (1999).
22. Beutel, T., Sárkány, J., Lei, G.-D., Yan, J. Y., and Sachtler, W. M. H., *J. Phys. Chem.* **100**, 845 (1996).
23. Komatsu, T., Ogawa, T., and Yashima, T., *J. Phys. Chem.* **99**, 13053 (1995).
24. Komatsu, T., Nunokawa, M., Moon, I. S., and Takahara, T., *J. Catal.* **148**, 427 (1994).
25. Chen, H.-Y., and Sachtler, W. M. H., *J. Catal.* **180**, 171 (1998).
26. Voskoboinikov, T. V., Chen, H.-Y., and Sachtler, W. M. H., *J. Mol. Catal. A* **155**, 155 (2000).
27. Chen, H.-Y., Wang, X., and Sachtler, W. M. H., *Appl. Catal. A* **194**, 159 (2000).
28. Ma, A. Z., and Grünert, W., *Chem. Commun.* **71** (1999).
29. Long, R. Q., and Yang, R. T., *J. Catal.* **188**, 332 (1999).
30. Long, R. Q., and Yang, R. T., *J. Am. Chem. Soc.* **121**, 5595 (1999).
31. Long, R. Q., and Yang, R. T., *J. Catal.* **194**, 80(2000).
32. Feng, X., and Hall, W. K., *J. Catal.* **166**, 368 (1997).
33. El-Malki, El-M., Van Santen, R. A., and Sachtler, W. M. H., *J. Catal.* **196**, 212 (2000).
34. Chen, H.-Y., El-Malki, El-M., Wang, X., Van Santen, R. A., and Sachtler, W. M. H., *J. Mol. Catal. A: Chemical* **162(1–2)**, 159 (2000).
35. Lobree, L. J., Hwang, I.-C., Reimer, J. A., and Bell, A. T., *J. Catal.* **186**, 242 (1999).
36. Hadjiivanov, K., Knözinger, H., Tsyntsarski, B., and Dimitrov, L., *Catal. Lett.* **62**, 35 (1999).
37. Hadjiivanov, K., Saussey, J., Freysz, J. L., and Lavalley, J. C., *Catal. Lett.* **25**, 103 (1998).
38. Szanyi, J., and Paffet, M. T., *J. Catal.* **164**, 232 (1996).
39. Laane, J., and Ohlsen, J. R., *Prog. Inorg. Chem.* **28**, 465 (1986).
40. Nakamoto, K., “Infrared Spectra of Inorganic and Coordination Compounds,” 2nd ed. Wiley, New York, 1970.
41. Anderson, L. A. H., Brandin, J. G. M., and Oderbrand, C. U. I., *Catal. Today* **4**, 173 (1989).
42. Stevenson, S. A., Vartuli, J. C., and Brooks, C. F., *J. Catal.* **190**, 228 (2000).
43. Anderson, L. A. H., Brandin, J. G. M., and Oderbrand, C. U. I., *Catal. Today* **4**, 187 (1989).
44. Ito, E., Mergler, Y. J., Nieuwenhuys, B. E., Calis, H. P. A., van Bekkum, H., and van den Bleek, C. M., *J. Chem. Soc., Faraday Trans.* **92**, 1799 (1996).